Adsorption 2, 111–119 (1996)

Piston-Driven Ultra Rapid Pressure Swing Adsorption

MOTOYUKI SUZUKI*, TAKANORI SUZUKI AND AKIYOSHI SAKODA
Institute of Industrial Science, University of Tokyo, 7-22-1 Roppongi, Minato-ku, Tokyo 106, Japan

JUN IZUMI
Nagasaki R&D Center, Mitsubishi Heavy Industries Ltd., 5-717-1 Fukahori-machi, Nagasaki 851-03, Japan

Received July 28, 1994; Revised September 18, 1995; Accepted October 24, 1994

Abstract. The piston-driven ultra rapid pressure swing adsorption (URPSA) equipment was developed and oxygen enrichment from air was examined as an example. The adsorbent bed is directly connected to the cylinder where a piston moves at high frequency. Thus pressurization and depressurization in the bed are driven by mechanical piston motion, which can achieve far more rapid cycles compared with the conventional pressure swing operation using valves. The cycle time is usually on the order of seconds or sub seconds. Oxygen enrichment from air up to about 60% or higher of oxygen concentration was achieved by small-scale equipment using zeolite 5A with a oxygen production capacity of 100 Nm^3-product gas/m^3-zeolite/hr, which is about ten times larger than those of commercialized PSAs for this purpose.

A simplified numerical model describing the mass transfer taking place in URPSA was developed. The model could simulate fairly well the air separation characteristics in terms of oxygen concentration, oxygen production capacity and oxygen yield. The proposed model helps in the understanding of the basic nature of URPSA and possible applications. This novel PSA is promising as a compact yet high-capacity PSA to be utilized in a wide variety of applications.

Keywords: pressure swing adsorption, bulk separation, experiments, simulation

Introduction

The development of compact and high-capacity separation processes is one of the most urgent requirements in such fields as carbon dioxide recovery from stack gases and oxygen enrichment for more efficient engine performance of automobiles. The pressure swing adsorption (PSA) process is a good candidate for achieving these purposes.

The production capacity of PSA must be improved for this purpose. This can be done by the development of more selective adsorbents, operation at low temperature where more adsorption capacity is expected (Sakoda and Suzuki, 1991), use of short cycle times where more throughput ratio is expected, etc. Among these approaches, the most dramatic improvement of capacity is expected to be achieved by rapid cycle operation. However, short cycle operation by conventional PSA processes is difficult because the lifetime of the ordinary valves employed is limited, affecting the continuous process operation of the process.

In this work, as a method to realize rapid operation of PSA, the piston-cylinder module employed in a conventional reciprocal engine equipment was used as the pressurizing and depressurizing mechanism and combined with an adsorption unit. Using this equipment, ultra-rapid operation was achieved and oxygen enrichment from air was experimentally tried. Moreover, a simplified numerical model was proposed to describe ultra-rapid pressure swing adsorption (URPSA)

*To whom all correspondence should be addressed.

operation. By simulation using this model, the basic characteristics of this operation can be formulated.

Basic Steps of Piston-Driven Ultra Rapid PSA

The URPSA equipment consists of a piston, a cylinder, valves and an adsorption bed. The piston is moved by an arm connected to the rotating disc driven by an electric motor. The basic operational steps are suction, adsorption and production, desorption, and exhaust steps, as shown in figure 1. The operation in each step is as follows:

Step 1: Raw gas is introduced into the cylinder while the piston goes down from the top position to the bottom position.

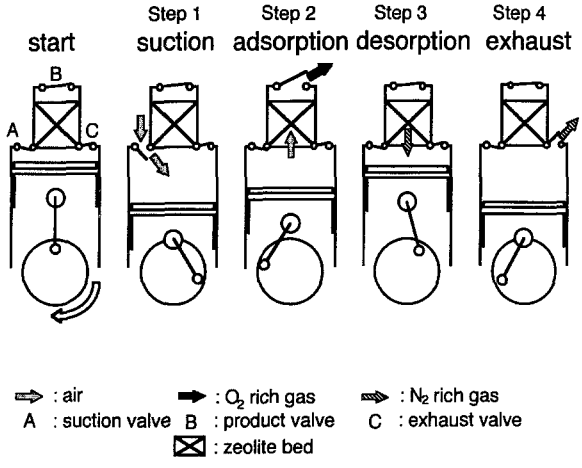

Figure 1. Sequence of piston-driven rapid cycle PSA for air separation.

Step 2: While the piston goes up, gas in the cylinder is compressed and introduced into the adsorbent bed, where adsorptive separation takes place and a less-adsorbable component is enriched in the product gas which is released from the top of the adsorbent bed.

Step 3: The piston goes down with all the valves closed. During this step, the depressurization and evacuation of the adsorbent bed take place. Desorption occurs and the cylinder is filled with the desorbed gas.

Step 4: In this step, the piston goes up again and the desorbed gas in the cylinder is removed as exhaust through the valve at the cylinder wall.

One adsorption-desorption cycle is completed with two up-and-down strokes of the piston. The cycle time in this sequential operation is controlled by the rotation speed of the motor and can be adjusted to seconds or sub seconds.

Experimental

Oxygen enrichment by using zeolite as an adsorbent was tried as an example of application. Oxygen is the less adsorbable component on zeolite 5A adsorbent.

Apparatus

A schematic diagram of the experimental apparatus is shown in figure 2. The cylinder diameter is 0.12 m. The piston stroke distance is 0.050 m; it gives displacement of 5.65×10^{-4} m^3 with one stroke. A packed bed of

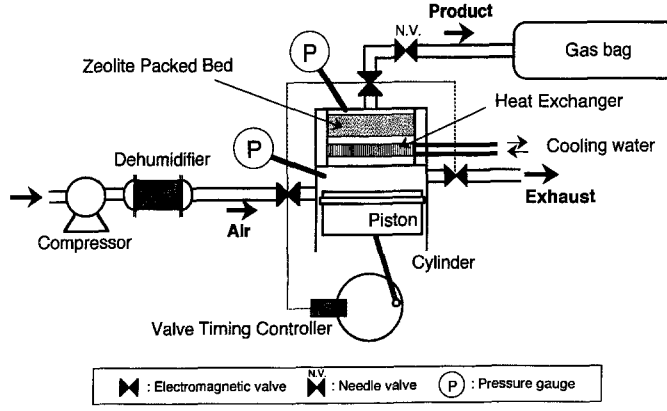

Figure 2. Experimental apparatus.

zeolite was placed at the upper part of the cylinder, the details of which are described later. Air introduced was dehumidified by passing through an activated alumina packed bed (*ca.* 5×10^{-3} m^3) to the dew point below 243 K before introduction to the cylinder. The product gas was released from the packed bed trough a needle valve and collected in a gas bag of 5×10^{-3} m^3 in volume after the process reached the dynamic steady state. A heat exchanger with square lattice openings for cooling the inlet gas was fabricated at the inlet of the adsorbent bed. Three electromagnetic valves were installed whose timings were controlled by using a personal computer (NEC, PC-9801 VX w/486). The delay time of the valve operation was within 12 ms. The pressure in the cylinder and the head space of the packed bed was monitored by pressure gauges (Copal Electronics, PA-8W) using the same personal computer.

Adsorption Unit and Adsorbents

Details of the adsorption unit are shown in figure 3. The packed of zeolite was 35 mm in height and 60 mm in diameter. The zeolite bed was fixed at the top and bottom by a sheet of filter paper (Advantech Toyo Filter Paper, No. 5A) and a stainless steel screen of 400 mesh size. Three copper-constantan thermocouples of 1.0 mm in sheath diameter were inserted into the center of the bed at the inlet, middle and outlet sections.

The adsorbent used was the popular zeolite 5A (Union Carbide Corporation) which was crushed and sieved into 48 to 80, 80 to 150 and 200 to 325 mesh size groups. As a preliminary treatment the zeolite was heated at 653 K for over 3 hours under evacuated conditions. The pretreated zeolite was carefully packed in the bed to avoid humidity uptake.

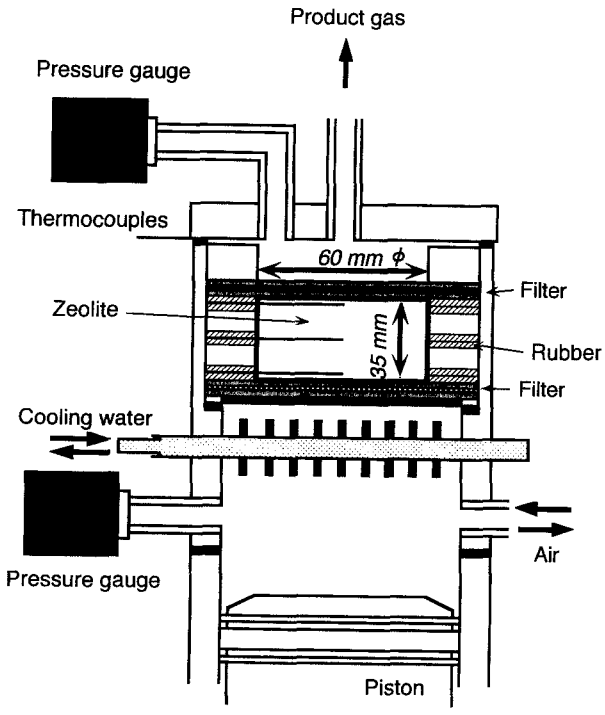

Figure 3. Details of adsorption column.

Procedures

The rotation speed of the motor was set to 80, 120, 160, 200 and 240 rpm corresponding, respectively, to cycle times of 1.5, 1.0, 0.75, 0.6 and 0.5 seconds. The oxygen concentration in the product gas collected in the gas bag was determined by an oxygen analyzer using zirconia (Toray Corporation, LC-100). The flow rates of the feed air and the product gas were measured with an integration type flowmeter (Shinagawa Manufacturing Co., Dp-2A-1). The temperature of the cooling water was keep constant at 278 K.

A Simplified Mathematical Model

Assumptions

The assumptions employed in the modeling of URPSA were as follows (Kowler and Kadlec, 1972; Jones and Keller II, 1980; Guan and Ye, 1992).

1) All gases are ideal.
2) Air is a mixture of nitrogen and oxygen only, and each gas is independent in terms of the adsorption equilibrium and rate.
3) The adsorption equilibrium is linear.
4) The adsorption rate is expressed by the linear driving force (LDF) approximation with a correction factor, Ω, due to rapid cyclic adsorption and desorption (Nakao and Suzuki, 1983).
5) The flow in the packed bed is the plug flow.
6) The Shape of the zeolite particle is spherical.
7) The pressure drop in the packed bed is represented by Ergun's equation (Ergun, 1952) as a first approximate.
8) The temperature of the entire system is constant at 303 K.

In addition, the experimental apparatus used in this work has a small amount of leakage through the space between the cylinder wall and the piston. This was taken into account by introducing a specific parameter determined by preliminary experiments.

Basic Equations

The model is a box model consisting of the cylinder, the zeolite bed divided into 10 boxes and the head space of the packed bed. The mass balance of each box is written as follows.

The mass balance in the cylicder is,

$$\frac{dP_{\text{cyl}}}{dt}V_{\text{cyl}} + P_{\text{cyl}}\frac{dV_{\text{cyl}}}{dt} = \frac{dN_{\text{cyl}}}{dt}RT \tag{1}$$

where

$$\frac{dN_{\text{cyl}}}{dt} = F_{\text{feed}} + F_{\text{in}} + F_{\text{exhaust}} \tag{2}$$

$$V_{\text{cyl}} = S_{\text{cyl}}x_{\text{pi}} \tag{3}$$

$$x_{\text{pi}} = \frac{x_{\text{pi max}} - x_{\text{pi min}}}{2}\{\cos(\omega t + \pi) + 1\} \tag{4}$$

P_{cyl}, V_{cyl}, R and T present the total pressure in the cylinder, the volume, a gas constant and the temperature, respectively. N_{cyl} is the amount of gas present in the cylinder. F_{feed}, F_{in} and F_{exhaust} are the flows of the feed gas, to the packed bed and of the exhaust gas, respectively. F_{exhaust} contains the leak from the cylinder as described before. S_{cyl} and x_{pi} represent the cross sectional area of the piston and the length between the piston head and the ceiling of the cylinder. $x_{\text{pi max}}$ and $x_{\text{pi min}}$ are maximum and minimum of x_{pi}. ω is the angular velocity.

The mass balance of component i in the jth box of the zeolite bed is given as;

$$\frac{dN_{\text{bed}\,i,j}}{dt} = (F_{\text{bed}})_{i,j-1}(F_q)_{i,j} + (F_{\text{bed}})_{i,j} \tag{5}$$

$N_{\text{bed}\,i,j}$ is the amount of gas present in the bed. $(F_q)_{i,j}$ are and $(F_{\text{bed}})_{i,j}$ the fluxes due to adsorption and desorption, and to the adjacent box, respectively.

Adsorption rate and equilibrium relation are written as;

$$\gamma\frac{dq_{i,j}}{dt} = (K_F a_v)_{i,j}\frac{(p_{\text{bed}})_{i,j} - (p^*_{\text{bed}})_{i,j}}{RT} \tag{6}$$

$$(K_F a_v)_{i,j} = \frac{\Omega_{i,j}(D_p)_{i,j}(1-\varepsilon)}{R_p^2} \tag{7}$$

$$q_{i,j} = (\beta_0)_i\frac{(p_{\text{bed}})_{i,j}}{RT} \tag{8}$$

$$(\beta_0)_i = \left(\beta_0^0\right)_i \exp\left(\frac{Q_{\text{st}}}{RT}\right) \tag{9}$$

where $K_F a_v$, D_p, ε, Q_{st} and (β_0^0) are the overall mass transfer coefficient, the pore diffusion coefficient, bed void fraction, the heat of adsorption and pre-exponent constant, respectively. $(p^*_{\text{bed}})_{i,j}$ is the pressure in equilibrium with the present amount adsorbed, $q_{i,j}$. $\Omega_{i,j}$ is a coefficient depending on $(\tau_c)_{i,j}$ (Nakao and Suzuki, 1983) given by;

$$(\tau_c)_{i,j} = \frac{(D_p)_{i,j}t_c}{R_p^2} \tag{10}$$

where t_c is the adsorption time and R_p is the radius of adsorbent particle.

D_p is evaluated as follows.

$$(D_p)_{i,j} = \frac{\varepsilon_p}{k^2}(D_0)_{i,j} \tag{11}$$

$$\frac{1}{(D_0)_{i,j}} = \frac{1}{(D_m)_{i,j}} + \frac{1}{(D_K)_i} \tag{12}$$

$$(D_K)_i = \frac{2}{3}r_a\sqrt{\frac{8RT}{M_i}} \tag{13}$$

where D_M and D_K are the molecular diffusion coefficient and the Knudsen diffusion coefficient, respectively.

ε_p is the particle void fraction, k^2 is the tortuosity factor, r_a is the macropore radius and M_i is the molecular weight of the ith component.

The mass balance in the head space is given as

$$\frac{dN_{\text{up}}}{dt} = (F_{\text{bed}})_{i,j\,\text{max}} + F_{\text{product}} \tag{14}$$

where N_{up} is the amount of gas present in the head space over the zeolite bed and F_{product} is the flow of the product gas.

Calculations

The calculation methods are as follows:

(1) The pressure change in the cylinder by the piston motion at time, t, was calculated.
(2) The amount of gas flowing from the cylinder into the first box of the zeolite bed was obtained.

Table 1. The characteristic parameters of zeolite used (Miller et al., 1987; Kawazoe et al., 1966).

Equilibrium constant, β_0^0	[—]	Nitrogen	1.75×10^{-5}
		Oxygen	1.30×10^{-5}
Heat of adsorption, Q_{st}	[cal/mol]	Nitrogen	4,040
		Oxygen	3,370
Macropore radius, r_a	[m]		0.47×10^{-6}
Bed void fraction, ε	[—]		0.4
Particle void fraction, ε_p			0.3
Tortuosity, k^2	[—]		3.4

(3) The pressure in the first box was calculated.
(4) The pressure decrease by adsorption was calculated.
(5) The flow to the next box, the second box, was evaluated according to pressure difference between the first box and second box by using the resistance calculated from Ergun's relation.
(6) The same procedure was repeated for the following boxes.

Sets of parameters are shown in Table 1 (Miller et al., 1987; Kawazoe et al., 1966). The particle radius, R_p, represent the average particle size.

Results and Discussion

Pressure Swings

Pressure changes at the inlet and outlet of the zeolite bed with cycle time are shown in figures 4(a), (b) and (c) for those cases where particles of 48–80, 80–150 and 200–325 mesh size were employed. The first quarter of the cycle time is the suction step when the piston descends from the upper dead point. The solid and dotted lines respectively present the pressure swings at the inlet and outlet of the zeolite bed. These were calculated using the model described above.

When smaller particles were used, smaller pressure changes at the outlet of the zeolite bed and larger at the inlet were found. Also, in figures 4(a)–(c), differences in phase lags between the pressure changes at the inlet and the outlet of the zeolite bed were observed for different particle sizes. These are caused by the different pressure wave propagations due to different conductance in the beds of different particle sizes.

This suggests that the separation performance depends greatly on particle size because the system pressure changes effective for adsorption and desorption are controlled by the pressure drop performances in the packing bed. And as compared with Rapid PSA (Turnock and Kadlec, 1971), larger pressure swing over and under the atmospheric pressure is achieved in a shorter cycle time.

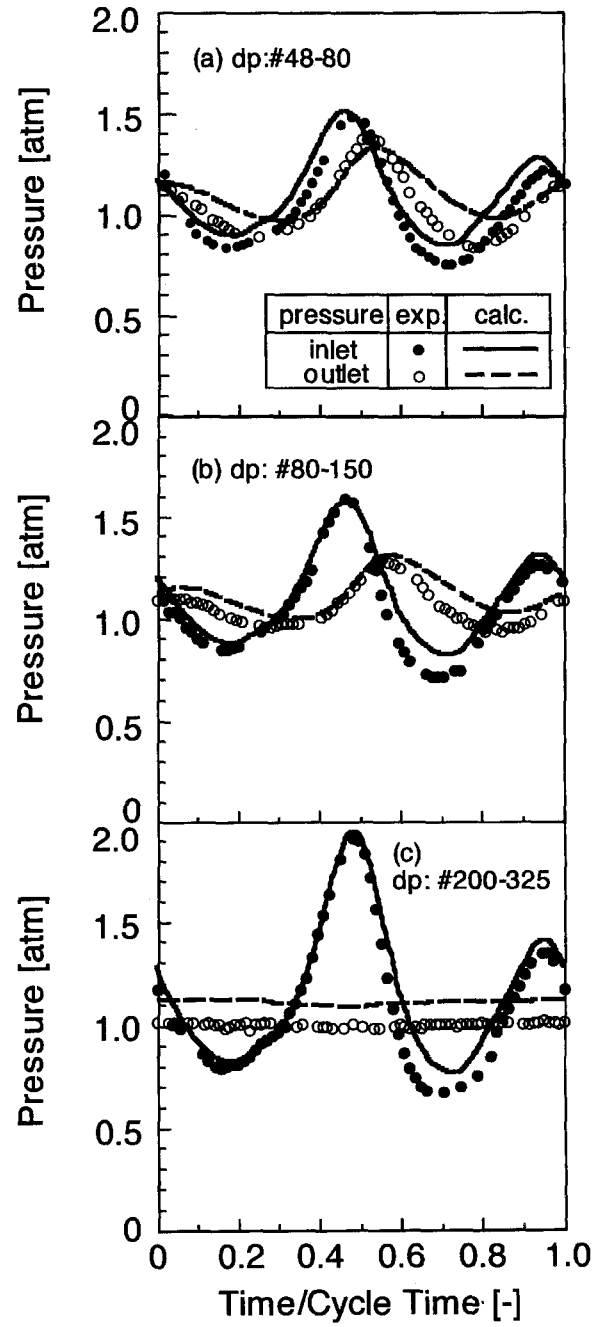

Figure 4. Pressure swing in adsorption bed, cycle time: 1.0 sec: (a) dp: #48–80, (b) dp: #80–150, (c) dp: #200–325.

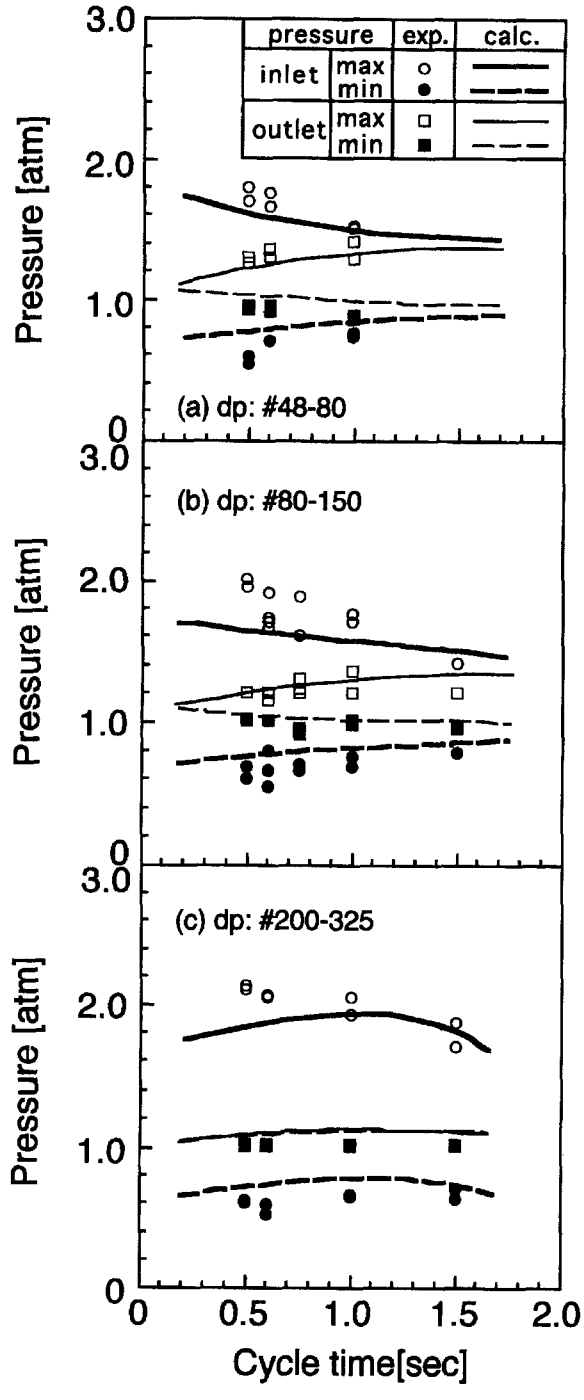

Figure 5. Change of maximum and minimum pressures during URPSA operations with cycle time: (a) dp: #48–80, (b) dp: #80–150, (c) dp: #200–325.

The pressure difference between the highest and the lowest pressures at the inlet and the outlet of the zeolite bed is shown in figures 5(a)–(c) as a function of cycle time. Apparently, in contrast to the normal PSA, the adsorption and desorption pressure varies with change in cycle time.

In figures 4(a)–(c), two peaks of pressure were found within one cycle. These peaks are considered to be a function of the flow resistance of the pipings and valves used in the experiments. There is thus still room for further improvement of the apparatus and the sequential mode of operation.

The pressure swings obtained from experiments and calculations were in good agreement.

Oxygen Concentration

The dependence of the oxygen concentration in the product gas on cycle time is showed in figure 6. The oxygen concentration was much dependent on the cycle time, since the pressure swing profile was controlled by the cycle time as mentioned before. The oxygen concentration also varied considerably with particle size of zeolite. The highest oxygen concentration was achieved when the particles of 80 to 150 mesh size were used. Although the optimization was not carried out at this stage, the importance of the selection of the most suitable particle size for achieving higher oxygen concentration is emphasized.

Also in these cases, simple simulations gave sufficiently good estimation of oxygen concentrations. Further improvement of experimental procedure and

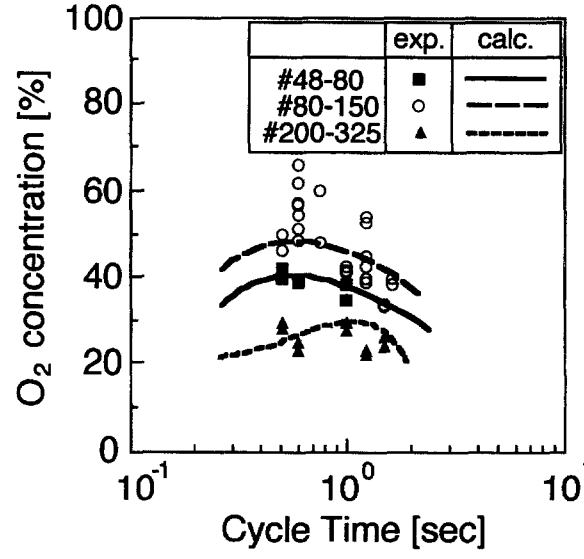

Figure 6. Dependency of oxygen concentration of cycle time.

modelling will be necessary if much better agreement needed in future works.

Capacities and Yield

Usually, the production capacity of PSA is defined as;

$$\text{Production Capacity [N-m}^3\text{-product gas/m}^3\text{-bed/hr]} = \frac{G_{\text{product}}}{V_{\text{bed}}} \quad (15)$$

A more meaningful capacity can be defined as the oxygen production capacity described by Eq. (16). In this definition, the PSA process is regarded as a pure-oxygen-production process and the product gas is the mixture of pure oxygen and air.

$$\text{Oxygen Production Capacity [N-m}^3\text{-oxygen/m}^3\text{-bed/hr]} = (1.26_6 C_{\text{product}} - 0.26_6)\left(\frac{C_{\text{product}}}{V_{\text{bed}}}\right) \quad (16)$$

where C_{product} are the oxygen concentration of the product gas, G_{product} is flow rate of product gas and V_{bed} is the bed volume.

The cycle time dependence of the oxygen production capacity is shown in figure 7. Since the oxygen production capacity of normal PSA is usually below 10 Nm^3-oxygen m^{-3}-bed hr^{-1}, the oxygen production capacity of the proposed URPSA can be about 10 times that of normal PSA. The highest oxygen production capacity was derived also when the particles of 80 to 150 mesh size were used.

Oxygen yield is defined in conventional form as follows:

$$\text{Oxygen yield [\%]} = \frac{\langle\text{Oxygen output}\rangle}{\langle\text{Oxygen input}\rangle} \times 100 = \frac{G_{\text{product}} C_{\text{product}}}{G_{\text{feed}} C_{\text{feed}}} \times 100 \quad (17)$$

The cycle time dependence of the oxygen yield is shown in figure 8. The oxygen yield of the URPSA in this experiment was less than 5%. It has become clear that the oxygen enrichment by this URPSA gives extremely high oxygen production capacity and low oxygen yield.

Simulations of this URPSA on the basis of the simple numerical model proposed in this work were satisfactory. Future investigation will involve the improvement

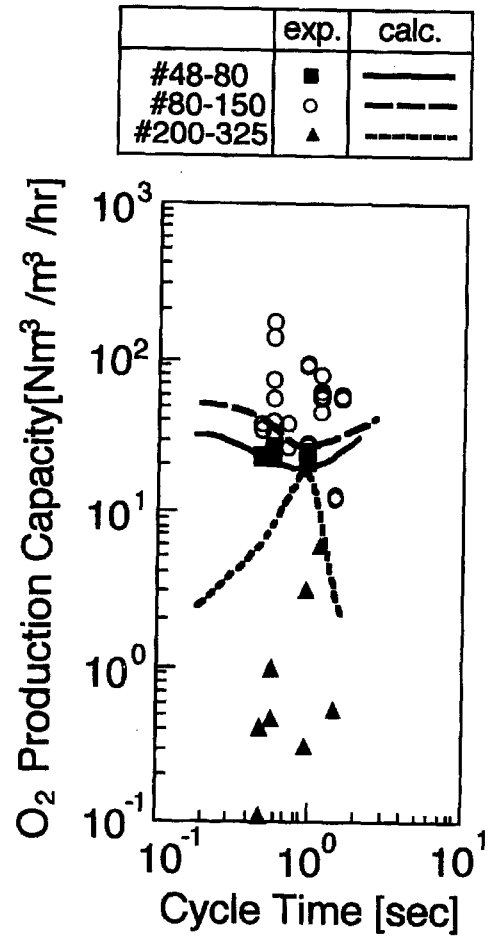

Figure 7. Dependency of oxygen production capacity on cycle time.

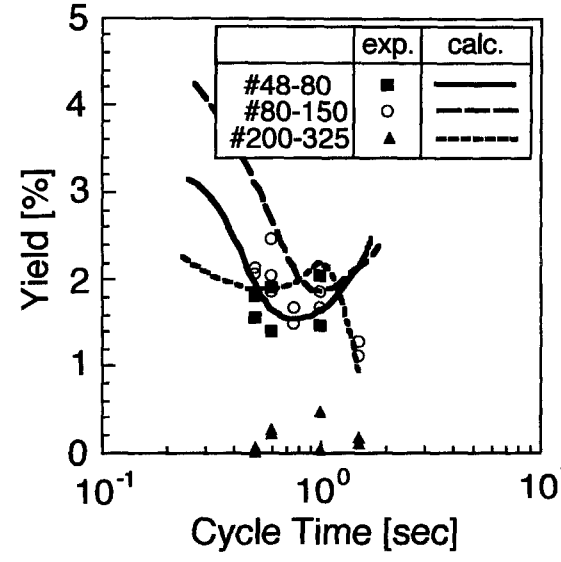

Figure 8. Dependency of oxygen yield on cycle time.

and optimization of the sequential operation mode. In this way, prediction of performance in novel applications becomes possible by numerical simulations.

Conclusion

The piston-driven ultra rapid pressure swing adsorption (URPSA) was developed and oxygen enrichment from air using zeolite was carried out. About 60% oxygen-enriched gas was produced with an oxygen production capacity of about 100 $Nm^3\ m^{-3}$-bed hr^{-1}, which was one order of magnitude higher than that obtained by commercialized oxygen-enrichment PSAs. However, oxygen yield was no higher than 5%. Oxygen enrichment by this URPSA gave extremely high oxygen production capacity and low oxygen yield. A simplified numerical model describing this URPSA was also proposed and numerical simulations using the model were compared with the experiment. This model will be useful for further investigations involving the improvement and optimization of cyclic operations and feasibility studies for application of this novel PSA.

Nomenclature

C	molar fraction	—
D_p	pore diffusion coefficient	m^2/s
D_0	constant defined by Eq. (12)	m^2/s
D_M	molecular diffusion coefficient	m^2/s
D_K	Knudsen diffusion coefficient	m^2/s
F	flow rate	mol/s
G	flow rate	m^3/hr
k^2	tortuosity factor	—
$K_F a_v$	overall mass transfer coefficient	l/s
M	molecular weight	kg/mol
N	amount of molecule	mol
p	partial pressure	Pa
P	total pressure	Pa
q	amount adsorbed	mol/kg
Q_{st}	heat of adsorption	J/mol
R	gas constant	J/mol/K
r_a	macropore radius	m
R_p	particle radius of adsorbent	m
S	cross sectional area	m^2
t	time	s
T	temperature	K
t_c	adsorption time	s
V	volume	m^3
x	length between piston head and cylinder ceiling	m

Greek letters

β_0	adsorption capacity coefficient	m^3/kg
β_0^0	pre-exponent constant in Eq. (9)	—
γ	packing density	kg/m^3
ε	bed void fraction	—
ε_p	particle void fraction	—
τ_c	defined by Eq. (10)	—
π	circular constant	—
ω	angular velocity	rad/s
Ω	constant given by τ_c	—

Subscripts

bed	in bed
cyl	in cylinder
exhaust	exhaust step
feed	suction step
i	component
in	between cylinder and bed
j	j-th box
max	maximum
min	minimum
pi	piston
product	product step
q	adsorption
up	head space

Acknowledgment

This work was partly supported by International Joint Research Grant of New Energy and Industrial Technology Development Organization (1993).

References

Ergun, S., "Fluid Flow Through Packed Columns," *Chem. Eng. Prog.*, **48**(2), 89–94 (1952).

Guan, J. and Z. Ye, "Optimization of the Operation Parameters for Rapid Pressure Swing Adsorption," *Fundamentals of Adsorption Proceedings of Fourth International Conference on Fundamentals of Adsorption*, 243–249 (1992).

Hart, J. and W.J. Thomas, "Gas Separation by Pulsed Pressure Swing Adsorption," *Gas Sep. Purif.*, **5**, 125–133 (1991).

Jones, R.L., G.E. Keller, and R.C. Wells, "Rapid Pressure Swing Adsorption Process with High Enrichment Factor," U.S. Patent No. 4, **194**, 892 (1980).

Jones, R.L. and G.E. Keller, "Pressure-Swing Parametric Pumping—A New Adsorption Process," *J. Separ. Proc. Technol.*, **2**(3), 17–23 (1981).

Kawazoe, K., I. Sugiyama, and Y. Fukuda, "On Effective Diffusivity in Porous Solids," *Kagakukogaku*, **30**, 1007–1012 (1966).

Kowler, D.E. and R.H. Kadlec, "The Optimal Control of a Periodic Adsorber: Part 1. Experiment," *AIChE Journal*, **18**(6), 1207–1219 (1972).

Miller, G. W., K.S. Knaebel, and K.G. Ikels, "Equilibria of Nitrogen, Oxygen, Argon and Air in Molecular Sieve 5A," *AICHE Journal*, **33**(2), 194–201 (1987).

Nakao, S. and M. Suzuki, "Mass Transfer Coefficient in Cyclic Adsorption and Desorption," *J. Chem. Eng Japan*, **16**(2), 114–199 (1983).

Pritchard, C.L. and G.K. Simpson, "Design of an Oxygen Concentrator Using the Rapid Pressure-Swing Adsorption Principle," *Chem. Eng. Res. Des.*, **63**, 467–471 (1986).

Rota, R. and P.C. Wankat, "Intensification of Pressure Swing Adsorption Processes," *AIChE Journal*, **36**(9), 1299–1312 (1990).

Sakoda, A. and M. Suzuki, "The Effects of Chilled Air Feed on Oxygen-Enrichment Pressure Swing Adsorption by Simplified Computer Simulation," *Sep. Tech.*, **1**, 73–77 (1991).

Skarstrom, C.W., *Recent Developments in Separation Science*, **2**, 95, N.N. Li (Ed.), CRC Press, Ohio, 1975.

Suzuki, M., *Adsorption Engineering*, 63–93, 156–167, 253–259, Kodansha, Tokyo, 1990.

Turnock, P.H. and R.H. Kadlec, "Separation of Nitrogen and Methane via Periodic Adsorption," *AIChE Journal*, **17**(2), 335–342 (1971).